



**Michigan
Technological
University**

Michigan Technological University
Digital Commons @ Michigan Tech

Michigan Tech Publications

9-7-2022

A Novel RID Algorithm of Muon Trajectory Reconstruction in Water Cherenkov Detectors

Neerav Kaushal
Michigan Technological University, kaushal@mtu.edu

Follow this and additional works at: <https://digitalcommons.mtu.edu/michigantech-p>



Part of the [Physics Commons](#)

Recommended Citation

Kaushal, N. (2022). A Novel RID Algorithm of Muon Trajectory Reconstruction in Water Cherenkov Detectors. *Astrophysical Journal*, 936(2). <http://doi.org/10.3847/1538-4357/ac8798>
Retrieved from: <https://digitalcommons.mtu.edu/michigantech-p/16405>

Follow this and additional works at: <https://digitalcommons.mtu.edu/michigantech-p>



Part of the [Physics Commons](#)



A Novel RID Algorithm of Muon Trajectory Reconstruction in Water Cherenkov Detectors

Neerav Kaushal

Department of Physics, Michigan Technological University, 1400 Townsend Drive Houghton, MI 49931, USA; kaushal@mtu.edu*Received 2022 April 5; revised 2022 July 29; accepted 2022 August 6; published 2022 September 7*

Abstract

Cosmic rays that strike the top of the Earth's atmosphere generate a shower of secondary particles that move toward the surface with relativistic speeds. Water Cherenkov detectors (WCDs) on the ground can detect charged muons, which are one of the many particles generated in the shower, with the Cherenkov imaging technique. A large number of these muons travel in WCD tanks near the speed of light in a vacuum, faster than the speed of light in water, and so trigger isotropic Cherenkov radiation, which is detected by the photomultiplier tubes (PMTs) placed inside the tanks. When the radial component of the speed of the muon toward a PMT drops from superluminal to subluminal, the PMT records Cherenkov light from an optical phenomenon known as relativistic image doubling (RID), which causes two Cherenkov images of the same muon to appear suddenly, with both images moving in geometrically opposite directions on the original muon track. The quantities associated with the RID effect can be measured experimentally with a variety of detector types and can be used to find various points on the original trajectory of the muon. In this paper, a detailed study of reconstructing the trajectory of a muon entering a WCD using the RID technique has been presented. It is found that the measurements of standard RID observables enables a complete reconstruction of the trajectory of the muon to a high degree of accuracy with less than 1% error.

Unified Astronomy Thesaurus concepts: [Cosmic ray showers \(327\)](#); [Special relativity \(1551\)](#); [Astronomical optics \(88\)](#)

1. Introduction

When a single high-energy particle like a gamma-ray photon strikes the top of the Earth's atmosphere, it produces a cascade of other particles which travel down toward the surface with relativistic speeds (Rossi 1933). This air shower consisting of a variety of charged and uncharged particles, also contains a charged muon whose lifetime is roughly 2.2 microseconds in its rest frame of reference (Tanabashi et al. 2018), but owing to its relativistic speed, this lifetime is dilated in the frame of reference of the Earth. Therefore, charged muons can reach the surface of the Earth without decaying.

These charged muons enter large tanks in water Cherenkov detectors (WCDs) that are made specifically to detect the former. Muons traveling faster than the speed of light in water trigger Cherenkov radiation (Čerenkov 1937), which can be observed by a number of detectors inside the tanks.

Recently, an optical phenomenon known as relativistic image doubling (RID) (Cavaliere et al. 1971; Nemiroff 2015, 2018, 2019) has gained much attention. With RID, objects moving superluminally in a medium (faster than the medium's speed of light) can appear twice simultaneously to an observer. When the radial speed of the muon toward a detector inside a WCD drops from superluminal to subluminal, two bright Cherenkov images of the muon suddenly appear and diverge. This nonclassical creation of images has been experimentally observed by Clerici et al. (2016) wherein the authors investigated the kinematic effects linked with the superluminal motion of a light source using high temporal resolution imaging techniques and found image pair annihilation and creation when the speed of the source toward the observer

dropped from superluminal to subluminal propagation regions. Furthermore, Velten et al. (2013) experimentally observed temporal inversion effects using light-in-flight (LiF) femtography and showed that in the single image visualization of a video of a laser pulse traveling through a bottle of a specific liquid, the events could appear to happen at incorrect timings and can also appear in the wrong temporal order. This could also create effects that could seem to move superluminally. Faccio & Velten (2018) provides a review of various time of flight distortions and relativistic effects observed by LiF photography techniques. The same RID effect has been hypothesized to help explain light curves in gamma-ray bursts (Hakkila & Nemiroff 2019). Recently, RID effects have been suggested to be commonly found in images of air showers by imaging atmospheric Cherenkov telescopes (IACTs) (Nemiroff & Kaushal 2020) and the Cherenkov images of muons in WCDs (Kaushal & Nemiroff 2020).

In this work, it is shown how this unique and interesting optical phenomenon can be used to reconstruct muon tracks completely in ground-based WCDs like those deployed by Auger (Aab et al. 2015), the High-Altitude Water Cherenkov (HAWC) observatory (BenZvi 2015), Kamiokande (Arisaka et al. 1984), and IceCube (Aartsen et al. 2017). It is shown that the trajectory of a muon traveling inside a WCD with a constant velocity can be completely reconstructed by extracting two points on its trajectory with at least three detectors observing an RID effect, given an independent measurement of the muon's velocity.

The paper is structured as follows. In Section 2, the conceptual basis of RID is reviewed briefly in relation to how it can be detected from inside a WCD. For a detailed discussion of the mathematical framework behind the concept, the reader is referred to Nemiroff & Kaushal (2020) and Kaushal & Nemiroff (2020). In Section 3, an RID algorithm for the reconstruction of a muon track starting from the top of the tank and ending at the tank floor,



Original content from this work may be used under the terms of the [Creative Commons Attribution 4.0 licence](#). Any further distribution of this work must maintain attribution to the author(s) and the title of the work, journal citation and DOI.

is developed mathematically using systems of nonlinear equations. In Section 4, a simulated trajectory of a muon entering a WCD tank similar to the tanks used in the HAWC observatory, is reconstructed. It is assumed that a typical WCD is equipped with a photomultiplier tube (PMT) that records brightness as a function of time and a digital camera that records brightness as a function of angular position (or a video detector that records both the brightness of the muon track and its angular position with time). In Section 5, different methods of further constraining the particle trajectory using the RID algorithm and the advantages of this technique are discussed.

2. RID: A Brief Review

Several RID concepts discussed in this section are followed from Nemiroff & Kaushal (2020). Consider a cosmic ray muon traveling with a speed $v > c_w$, where c_w is the speed of light in water, and entering a WCD tank filled with water up to height H . It enters the top of the tank at time $t=0$ through point A and leaves the bottom of the tank through point B . The muon is assumed to be at a constant speed v throughout the tank.

As soon as the muon enters the tank, it causes the emission of isotropic Cherenkov radiation around its track in a cone, which is observed by detectors placed at the bottom of the tank, as its ‘‘Cherenkov image’’. A detector inside the advanced Cherenkov cone of the muon will observe the phenomenon of RID. From the point of view of such a detector, the muon will first traverse a path starting from its entry point A (see Figure 1) in the tank down to a height z_C from the bottom of the tank, where the radial component of its speed toward the detector (v_r) equals the speed of light in water (c_w). In this region of the track, the radial speed of the muon toward the detector is *faster* than the speed of the Cherenkov radiation it causes. So, this region of the muon track will be seen by the detector time-backwards, i.e., the Cherenkov radiation emitted increasingly earlier along the muon track will reach the detector at increasingly later times. This happens because the emissions of the muon precede the muon itself in this region and therefore, this part of the track will appear to go *up* from height z_C along the track. After the muon has descended down past z_C , its radial speed toward the detector will be *slower* than its Cherenkov light, so this region of the muon track will appear normally to the detector, i.e., the muon will appear to travel down toward the exit point monotonically with time. Therefore, the detector first observes the muon at height z_C on its track and *not* at the point of its entry in the tank. After the muon is first seen at z_C , it is simultaneously seen at two locations on its original track, one below and other above z_C .

Note that a detector outside the Cherenkov cone of the muon will not observe an RID effect because the radial speed of the muon toward this detector is always subluminal, even though the total speed of the muon is always superluminal. For such a detector, the muon will appear to travel from entry point A to exit point B classically.

The detector is located at the floor of the tank at D , a distance L from the point of entry A and M from the point of exit B . The path length of the muon in the tank is given by $\frac{H}{\cos \theta}$, where θ is the angle between the muon path and the vertical. The height of the muon from the ground at any time t during its course in the tank is given by z . This is shown in Figure 1.

The time taken by the detector to observe the muon since the muon entered the tank is given by t_{total} , which can be written as the sum of two times. The first is the time taken by the muon to

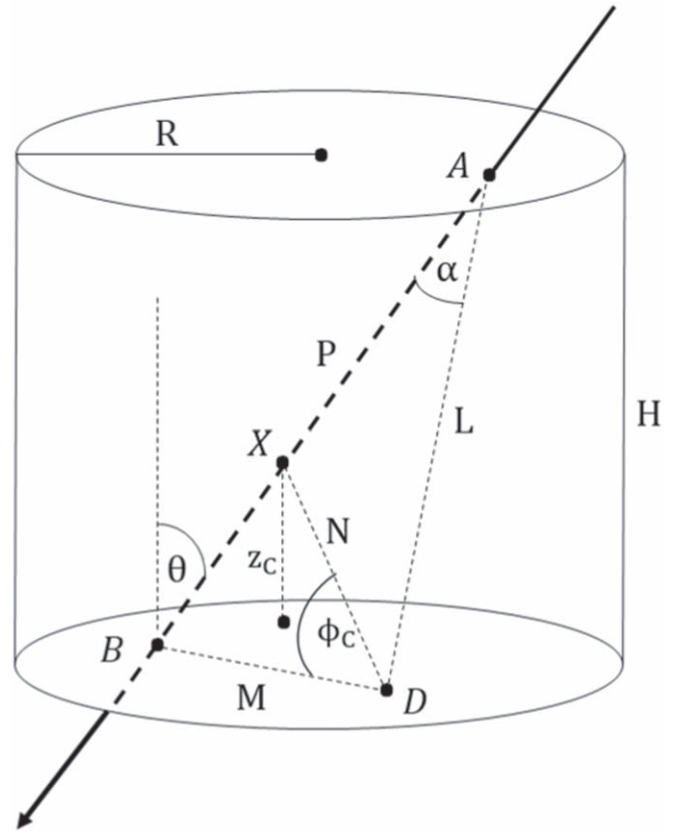


Figure 1. A muon enters the top of a WCD tank through A and leaves through the bottom at B . The path length of the muon inside the tank is given by $P (=H/\cos \theta)$ while the distances of the detector D from A and B are given by L and M , respectively (Kaushal & Nemiroff 2020).

descend down to a location which is at height z from the ground, t_{descend} and the second is the time taken by the light to reach from that location at height z to the detector, $t_{\text{radiation}}$. The ‘‘critical height’’ where the muon is first seen by the detector is given by z_C and it occurs at a time t_{min} , when t_{total} is a minimum. This can be found by solving $dt_{\text{total}}/dz = 0$ for z (Nemiroff & Kaushal 2020). For a muon entering the tank from the top and leaving through the bottom, z_C is given by

$$z_C = H - \left(L \cos \alpha - \frac{c_w L \sin \alpha}{\sqrt{v^2 - c_w^2}} \right) \cos \theta, \quad (1)$$

where α is the angle between the detector and the muon track through point A . The ‘‘critical angle’’, ϕ_C , corresponding to the critical height z_C , where the muon is first seen by the detector, is the angle between the line joining the detector D with the point X of the critical height on the muon path (i.e., DX) and the line joining the detector with the exit point B of muon at the WCD floor (i.e., BD). ϕ_C is given by

$$\phi_C = \arccos \left(\frac{(P^2 + L^2 + M^2) \cos \theta + 2L \cos \alpha (z_C - P \cos \theta) - 2Pz_C}{2M \cos \theta \sqrt{L^2 - 2L \cos \alpha (P - \frac{z_C}{\cos \theta}) + (P - \frac{z_C}{\cos \theta})^2}} \right). \quad (2)$$

where P is the path length of the muon inside the tank (See Figure 1).

After t_{\min} , two images of the muon are observed simultaneously by the detector at heights z_{\pm} from the ground and angular locations ϕ_{\pm} wrt the detector–exit point line (i.e., BD). Once the height and time of each image of the pair is known, their apparent brightness can be calculated using their transverse velocities (Nemiroff & Kaushal 2020).

3. Reconstruction of the Muon’s Trajectory: Algorithm

Consider a muon entering a WCD tank from the top through point A with coordinates (x_A, y_A, H) and leaving from the bottom through point B with coordinates $(x_B, y_B, 0)$. The tank contains four detectors at the bottom arranged in a Y-pattern as shown in Figure 2. We only require a minimum of three detectors to develop the mathematical formulation for reconstruction of the trajectory. Consider detectors D_1, D_2 , and D_3 at locations $(x_{D1}, y_{D1}, 0)$, $(x_{D2}, y_{D2}, 0)$, and $(x_{D3}, y_{D3}, 0)$, respectively. These detectors are assumed to be inside the advanced Cherenkov cone of the muon and therefore, all three of them will observe an RID effect.

A detector here is considered to be a combination of a PMT which records the brightness and time of the muon’s trajectory and a video detector tracking both the angular position and brightness in time. Instead of a video detector, a digital camera could also be used as a static detector providing a record of brightness and angular location of the muon.

In order to completely reconstruct the trajectory of the particle, at least two points on its track need to be estimated. Consider the triangle ABD between a detector and the entry and exit points of the muon in the tank (Figure 1).

A system of three nonlinear equations can be set up for each detector as follows,

$$\left. \begin{aligned} \sqrt{L^2 + M^2 - 2LM \cos \phi_i} &= \frac{H}{\cos \theta} \\ \sqrt{M^2 + N^2 - 2MN \cos \phi_C} &= \frac{z_C}{\cos \theta} \\ \sqrt{L^2 + N^2 - 2LN \cos(\phi_i - \phi_C)} &= \frac{H - z_C}{\cos \theta} \end{aligned} \right\}, \quad (3)$$

where the critical height z_C , the critical angle ϕ_C , and the angle between the entry and exit point of the muon through the detector, $\phi_i (= \angle ADB)$, are the RID observables that can be measured experimentally. The angle θ can be written in terms of lengths M and N and can be computed from the light curve of the muon and an independent measurement of its velocity. This will be calculated for the example case of a muon entering a HAWC-like WCD in the next section.

This system of Equations (3) has a unique solution for the parameters L, M , and N which are then evaluated for each pair of detectors, i.e., $(L_i, M_i, N_i, L_j, M_j, N_j) \forall (i,j) = (1,2), (1,3), (2,3)$.

Now, for any single detector system, say $D_1 - D_2$, a system of four nonlinear equations with four unknown variables (x_A, y_A, x_B, y_B) can be set up to find the coordinates of points A and B , as follows,

$$\left. \begin{aligned} (x_A - x_{D1})^2 + (y_A - y_{D1})^2 + H^2 &= L_1^2 \\ (x_B - x_{D1})^2 + (y_B - y_{D1})^2 &= M_1^2 \\ (x_A - x_{D2})^2 + (y_A - y_{D2})^2 + H^2 &= L_2^2 \\ (x_B - x_{D2})^2 + (y_B - y_{D2})^2 &= M_2^2 \end{aligned} \right\}. \quad (4)$$

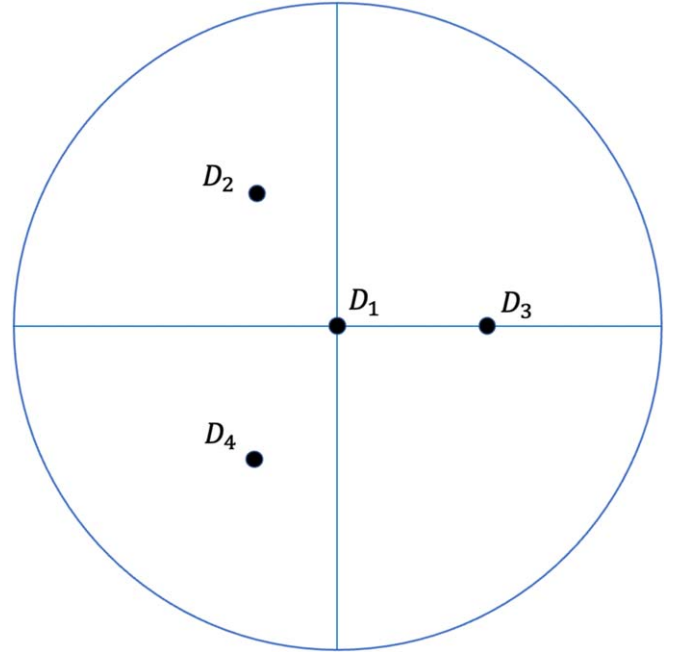


Figure 2. A top view of the WCD water tank. The three detectors D_2, D_3 , and D_4 are arranged in an equilateral triangle with detector D_1 at the circumcenter of the triangle. Only detectors D_1, D_2 , and D_3 will be considered for the reconstruction of the muon’s trajectory.

Solving the above system of equations for one detector system gives a number of possible values of coordinates of A and B , because there are more than one A and B pairs that can have the same lengths L, M , and N . The actual coordinates of A and B and thus the correct muon trajectory can be completely extracted by solving system (4) for the other two detector systems, i.e., $D_1 - D_3$ and $D_2 - D_3$ and the actual coordinates are the ones that are common to all the detector pairs. In general, the more the detectors, the higher the precision on the constraints of the muon’s trajectory. With four detectors, six possible detector pairs can be formed that are sufficient to pinpoint the coordinates to a very high degree of precision.

4. Reconstruction of the Muon’s Trajectory: Example

In this section, a simulated trajectory will be reconstructed for a muon incident on a HAWC-like WCD tank from the top at A and exiting through B , making some angle θ to the vertical. The light curve for the muon in this case is shown in Figure 3. The height of the water level in the tank, H , is 4.5 m and the four detectors are placed at the bottom of the tank in a Y-pattern (Sandoval 2013).

It can be seen from Figure 3 that only three of the four detectors will see an RID effect. The dashed curve represents that Cherenkov image of the muon which is going downwards along the original muon track up to the exit point B while the solid curve represents the Cherenkov image going up toward the entry point A .

For a detector observing an RID, the total time duration of the dashed curve is given by

$$\begin{aligned} \Delta t_{\text{dashed}} &= \left(\frac{AB}{v} + \frac{BD}{c} \right) - \left(\frac{AX}{v} + \frac{DX}{c} \right) \\ &= \frac{z_C}{v \cos \theta} + \frac{M - X}{c}, \end{aligned} \quad (5)$$

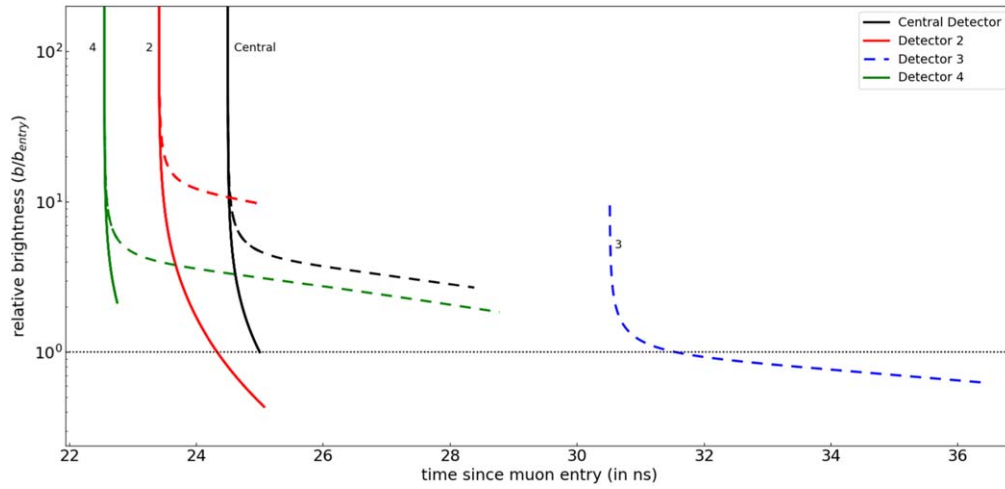


Figure 3. Light curve of a muon entering the WCD from the top and leaving through the bottom of the tank. The brightness on the y-axis is normalized wrt the brightness at the entry point as seen by the central detector. The dashed curve represents the Cherenkov image of the muon going toward the exit point B on the ground while the solid curve represents the image going up toward the entry point A .

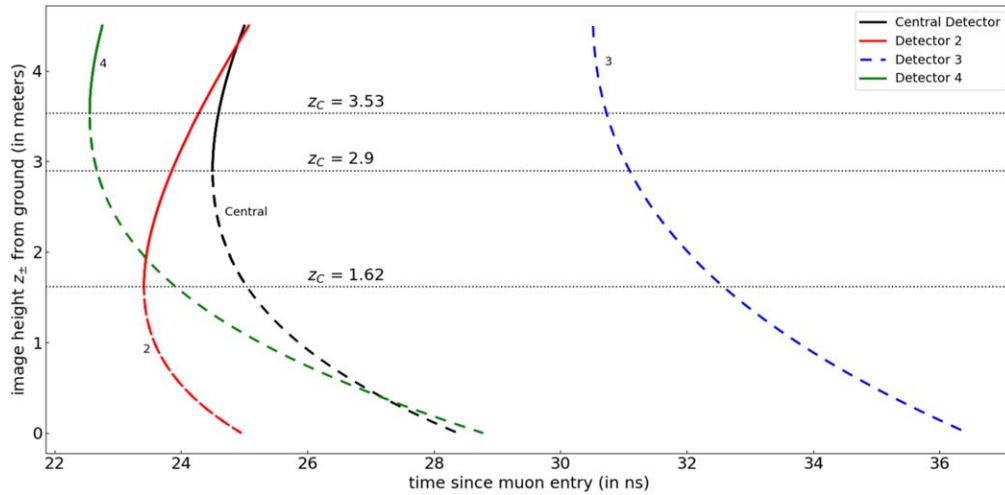


Figure 4. A graph of image height vs. the total time elapsed since the entry of muon in the tank. Note that for detector 3, there is no value of z_c inside the tank. Therefore, detector 3 is not inside the Cherenkov cone and will not observe an RID event.

and therefore, the value of $\cos \theta$ is

$$\cos \theta = \frac{c z_c}{v (c \Delta t_{\text{dashed}} + X - M)}. \quad (6)$$

Plots of the heights and angular locations of the Cherenkov images of the muon versus the total time since the entry of muon in the tank, corresponding to the light curve shown in Figure 3, are shown in Figures 4 and 5, respectively. These plots are generated for the case of a muon incident at an angle using the RID code (Kaushal & Nemiroff 2020).

A number of parameters that can be derived from these plots and can be experimentally measured, along with their values for the example case considered in this section, are listed in Table 1. The value of v can be obtained by an independent measurement of the Cherenkov angle of emission of the muon using standard methods employed in various Cherenkov detector systems. All the other parameters except the unknowns can be obtained by the measurement of RID observables.

Solving the system of Equations (3) yields the values of L , M , and N for the three detectors which represent the detector–entry point distance (D_iA), the detector–exit point distance (D_iB) and the

detector–critical height distance (D_iX), respectively. These are shown in Table 2.

The values of L and M for the three detectors are subsequently put in the system of Equations (4) to obtain several sets of solutions for the coordinates of A and B of the muon representing the possible trajectories. The correct solutions are the ones common to all the three detector pairs. The resulting coordinates of A and B are averaged over the three detector systems and are shown in Table 3. The significance of N is discussed in the next section.

It is seen from the table that the estimated values for the coordinates of the entry and exit point of the muon are very close to the actual values generated with simulations and the percentage error in extracting the coordinates is less than 1% in this case. Thus, the two points on the muon track are completely extracted with the measurements of observables of a typical RID phenomenon, which enables a complete reconstruction of the trajectory of the muon. The precision of the measurements of RID quantities, in turn, helps in further constraining this trajectory to a higher precision.

It is to be noted that in order for the detectors to observe the RID event, the critical height (z_c) for each detector should be

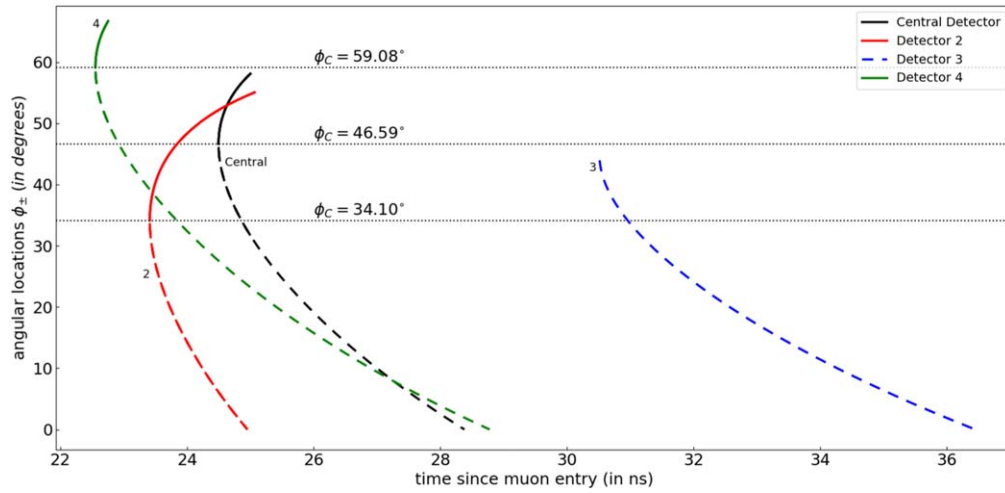


Figure 5. A plot of angular location vs. the total time for the Cherenkov images of the muon. Different detectors see the muon for the first time at different critical angles corresponding to different critical heights from the ground.

less than the height of the water tank as the detector could only observe the events occurring inside the volume of the tank. It follows, therefore,

$$0 < z_{Ci} < H \text{ or,} \\ \frac{-P_i}{L_i} < \frac{\sin \alpha_i}{\sqrt{q^2 - 1}} - \cos \alpha_i < 0,$$

where $q = v/c_w > 1$ and i denotes the detector number. For the case where the muon enters the tank from the top and leaves from the bottom or vice-versa, this solves to,

$$\sec \alpha_i < q < \frac{\sec^4\left(\frac{\alpha_i}{2}\right)(L_i^2 + P^2 - 2L_i P \cos \alpha_i)}{\left((L_i + P)\tan^2\left(\frac{\alpha_i}{2}\right) - L_i + P\right)^2},$$

$$\text{for } P < L_i \cos \alpha_i, \quad \alpha_i \in \left(0, \frac{\pi}{2}\right),$$

or

$$\sec \alpha_i < q < \frac{M_i}{|P - L_i \cos \alpha_i|},$$

$$\text{for } P < L_i \cos \alpha_i, \quad \alpha_i \in \left(0, \frac{\pi}{2}\right), \quad (7)$$

and

$$\sec \alpha_i < q, \quad \text{for } P \geq L_i \cos \alpha_i, \quad \alpha_i \in \left(0, \frac{\pi}{2}\right). \quad (8)$$

Inequalities 7 and 8 give the muon velocity constraints for which the detectors will observe the RID event and these constraints also agree with the simulations. Thus, the RID observations can also independently constrain the velocity of the muon and can be used as an additional method to check against the standard muon velocity estimation techniques currently used in WCDs.

For a detector to observe RID, the distance (x) traveled by the muon after entering the tank should be less than the distance at which the RID event occurs. This distance depends on the interplay of the velocity (v) of the muon and the time resolution of the detector. Given that the velocity of the muon entering the WCD tank follows some distribution, it is straightforward to calculate the time resolution that would

provide the minimum spatial resolution on the muon path that could be observed by the detectors. Our simulations for the muon's velocity used in Table 1 show that a detector having a time resolution lower than 10 ns (i.e., timesteps higher than 10 ns) will not be able to observe any RID event. This, though, does not mean that the RID event does not occur for that detector. It simply means that that particular detector will not be able to observe the RID event for lower resolutions, because the muon will already be outside the tank before the detector measures the associated observable at the next time step. The systematic error of reconstruction of the muon's trajectory is thus of the order of the time resolution of the detector, which in our example case is 10 ns. This time resolution will be higher for muons traveling closer to (and obviously higher than) the speed of light in water than the ones traveling with speeds much higher than the speed of light in water. A detailed discussion on various detector types and their time resolutions is provided in the next section. On the other hand, as evident from inequalities 7 and 8, there exist upper and lower velocity bounds for particular muon trajectories such that for muons traveling with speeds outside those bounds, the detector will never observe the RID, no matter how high the resolution. This is due to the fact that the RID for these muon trajectories occur at locations that are outside the water tanks, thus inaccessible to be observed by the detectors.

5. Discussion

As we have seen, the complete trajectory of a muon can be reconstructed from experimentally measured RID observables like the critical height z_C , the critical angle ϕ_C , etc. A minimum of three detectors observing an RID are required for this reconstruction. To constrain further the muon's trajectory to very precise values, the system of Equations (3) can be solved for at least four detectors observing an RID followed by solving a nonlinear system of twelve equations given by,

$$\left. \begin{aligned} (x_A - x_{Di})^2 + (y_A - y_{Di})^2 + H^2 &= L_i^2 \\ (x_B - x_{Di})^2 + (y_B - y_{Di})^2 &= M_i^2 \\ (x_{Xi} - x_{Di})^2 + (y_{Xi} - y_{Di})^2 + z_{Ci}^2 &= N_i^2 \end{aligned} \right\} \forall \quad i = 1, 2, 3, 4, \quad (9)$$

Table 1
A List of all Parameters and Their Values for the Example Muon Incidence of Section 4

Parameter	Value (SI units)	Description
H	4.5	Height of the WCD tank
x_A, y_A, z_A	Unknown, Unknown, H	Coordinates of the muon entry point A
x_B, y_B, z_B	Unknown, Unknown, 0.0	Coordinates of the muon exit point B
x_{D1}, y_{D1}, z_{D1}	0.0, 0.0, 0.0	Coordinates of detector D_1
x_{D2}, y_{D2}, z_{D2}	-0.925, 1.602, 0.0	Coordinates of detector D_2
x_{D3}, y_{D3}, z_{D3}	1.85, 0.0, 0.0	Coordinates of detector D_3
z_{C1}	2.896	Critical height for detector D_1
z_{C2}	1.618	Critical height for detector D_2
z_{C3}	3.530	Critical height for detector D_3
ϕ_{C1}	0.813	Critical angle for detector D_1
ϕ_{C2}	0.595	Critical angle for detector D_2
ϕ_{C3}	1.031	Critical angle for detector D_3
ϕ_{i1}	1.014	Angle between the entry and exit point through detector D_1
ϕ_{i2}	0.961	Angle between the entry and exit point through detector D_2
ϕ_{i3}	1.164	Angle between the entry and exit point through detector D_3
$\Delta t^{\text{dashed}1}$	3.88	Time for which the Cherenkov image going downwards from z_{C1} is visible to detector D_1
$\Delta t^{\text{dashed}2}$	1.54	Time for which the Cherenkov image going downwards from z_{C2} is visible to detector D_2
$\Delta t^{\text{dashed}3}$	6.23	Time for which the Cherenkov image going downwards from z_{C3} is visible to detector D_3
c_{vacuum}	3.0×10^8	Speed of light in vacuum
c_w	$c_{\text{vacuum}}/1.33$	Speed of light in water
v	c_{vacuum}	Speed of muon in water

Note. The objective is to find the unknown coordinates of the muon entry and exit points. The systems of nonlinear Equations (3) and (4) are solved to obtain a measure of L , M , and N for each detector first, and then the values of the unknown parameters depicting the coordinates of A and B .

Table 2

Solutions for the System of Equations (3) for Each of the Three Detectors

Parameter	Value
L_1, M_1, N_1	5.6362, 2.7968, 4.2393
L_2, M_2, N_2	5.6460, 2.0217, 2.9679
L_3, M_3, N_3	5.1384, 2.8906, 4.3154

Note. L is the distance between the detector and the muon entry point A , M is the distance between the detector and the muon exit point B , and N is the distance between the detector and the point X at critical height z_C where the muon is first observed by that detector. These values are fed to the system of Equations (4) to extract the coordinates of the muon entry point A and exit point B .

where i represents a single detector. This system of equations, when solved within some error tolerance, will give six points on the path of the muon's trajectory.

One of the many parameters involved in the working of the RID technique that can quantify the detectability of the muon's trajectory are θ (the angle between the muon's trajectory and the vertical) and ϕ_i (the angle between the entry and exit point of the muon through the detector). The current methods of estimation of the muon's trajectory in WCDs (Huentemeyer et al. 2009; Joshi 2019; Aisher 2016; Dingus 2007) use a completely different algorithm that also involves an independent estimation of the muon's velocity in the WCD tank, which is another parameter in our reconstruction method. One of the assumptions of the RID technique is that this muon's velocity is constant during the entire muon track across the WCD.

It should be noted that the RID method fails to work if no detector observes the RID event or if no more than two detectors observe the RID event. Though, it has been shown by Kaushal & Nemiroff (2020) using two separate simulation algorithms, that of all the muons entering the WCD, between

Table 3

The Solutions for the System of Equations (4)

Parameter	Results				Actual Values	Error
	$D_1 - D_2$	$D_2 - D_3$	$D_1 - D_3$	Mean		
x_A	2.3873	2.3746	2.3848	2.382	2.400	0.75%
y_A	2.4120	2.4244	2.4222	2.420	2.400	0.83%
x_B	0.7820	0.7808	0.7816	0.781	0.787	0.76%
y_B	2.6853	2.6856	2.6859	2.686	2.684	0.07%

Note. Columns 2 to 4 are the coordinates of A and B obtained from each possible pair of detectors. Column 5 and 6 contain the mean values and the actual simulated values pertaining to the light curves of the muon's trajectory, respectively. Finally, the last column contains the percentage errors of the results.

85% and 90% will be observed to trigger an RID event by at least one detector, thus indicating that it should be very common for HAWC-like WCDs to observe RID events.

As the images of the muon after the RID event fade within a few nanoseconds, it might seem that these light curves are practically immeasurable. However, the increasing frame rate of capturing images, attributed to computer technology and miniaturization, have resulted in imagers that are able to capture sub-nanosecond events (Clerici et al. 2016). First, there are hybrid pixel detectors which are fast time-stamping cameras sensitive to optical photons, such as MAPS-based PImMS-1 and PImMS-2 with a 12.5 ns resolution, a CMOS-based TimepixCam with a 10 ns resolution, and a Hybrid CMOS-based Tpx3Cam with a 1.6 ns resolution (see Nomerotski (2019) for a full review). Second, there are numerous microchannel plate-based photomultiplier tubes (MCP-PMTs) whose time response can be as fast as 100 picoseconds FWHM with a gain of up to 10^7 (Milnes et al. 2012). To observe small

events in close temporal proximity to much larger signals, the response of MCP-PMTs can be gated with an on/off ratio of up to 10^{13} in just 2 ns. It is worth noting that Hamamatsu's PMTs (that are currently employed in HAWC detectors) models R3809U-(50,51,52,53) have a response time of 1.2 ns and can very easily observe the RID event duration, even in the case of the fast dimming phase. These technological innovations raise the possibility of placing video detectors inside WCDs that can resolve RID events in both time and angle. Alternatively, simple digital cameras may be placed that can resolve the Cherenkov images only in angle, leaving the temporal resolution to the PMTs.

Using the trajectory representing the fast dimming phase (or the muon image that seems to go along the original muon direction) is one of the two trajectories that can be independently used for the reconstruction. Another method to improve the estimation of the trajectory is to use the slow dimming trajectory, i.e., the muon light curves for the Cherenkov image going upwards (solid curves in Figure 3). The same algorithm when applied to the Cherenkov images going upward will give more sets of values for the coordinates of A and B , further decreasing the error in the final estimates, enabling a much more precise trajectory. This has not been done in this work as the goal of this work is to introduce just how the RID technique can be used for this reconstruction with the least amount of information that could possibly be extracted from the RID events.

The RID technique has a number of advantages over the traditional reconstruction methods currently employed in WCDs. First, only three detectors observing an RID are needed to reconstruct the muon's trajectory unlike numerous PMTs currently employed in various WCD facilities around the world. Additional PMTs will only increase the precision of the reconstruction. Second, the RID method can be used as an independent technique to constrain muon velocities and can be used as a check against the traditional methods for estimating muon velocities. Third, the RID reconstruction method is a much more generalized algorithm that can be employed in other Cherenkov detection principles (such as IACT imaging and ring-imaging Cherenkov (RICH) detector systems) that usually employ different techniques of reconstruction after the detection of Cherenkov photons by PMTs.

There are also some limitations and complexities associated with the RID technique. First, as the detector itself is an extended structure and not a point, its large size might result in the light travel time across its surface being significant when compared to the time taken by the Cherenkov light to reach the detector. Then, any light curve that a PMT measures will convolve the size and shape of the PMT, not just the geometry inherent to the muon's path. Second, because RID events are observer-dependent even for the same muon's trajectory, the locations of the detectors are very important. Simply adding together the brightness of different images from multiple PMTs, at the times of the brightness measurements, for example, will typically convolute RID effects beyond recognition. However, a careful reconstruction accounting for the timing of separate RID events as seen by different detectors should be possible that could enhance RID detection and better determine the muon's real track inside the WCD (Nemiroff & Kaushal 2020).

The RID algorithm can independently confirm the information about the muon's trajectory, including the brightness along its path. When combined with the standard algorithms used at WCD systems for the reconstruction of the Cherenkov cone, it

can greatly constrain the muon's trajectory with much smaller errors. This, in turn, can reduce the cost of construction, maintenance, and working of a very large number of detectors usually deployed in such systems.

The same RID algorithm can also be used in IACTs to reconstruct the trajectories of the secondary charged particles in the air showers. This can greatly reduce the number of telescopes used in systems and provide much better directional estimates of the shower.

In summary, the RID method is a novel reconstruction algorithm that provides a highly accurate, simple, and effective technique to reconstruct the trajectories of muons in WCDs and can greatly reduce the number of detectors used in typical WCD systems.

6. Future Impacts

Various WCD systems around the world use thousands of PMTs (11,129 PMTs in the Super-Kamiokande detector in Japan, for example) in order to detect Cherenkov radiation emitted by muons from the cosmic air showers entering the water tanks. Cherenkov detection is based on the simple fact that the greater the accuracy of reconstructing the air shower's trajectory, the better the pinpointing of the source of the cosmic/gamma-rays. This work presents an entirely new technique to reconstruct the same shower trajectory in a much simpler manner. It shows that no more than three PMTs observing an RID are needed to extract the complete muon's trajectory within a percent level accuracy, and increasing this number to four, five, or six PMTs will only increase the accuracy of the reconstruction, and reduce the manufacturing and installation costs of numerous highly expensive PMTs. This work can also serve as a standard theoretical check against the experimentally extracted muon trajectories in WCDs.

I believe that the RID reconstruction method may have the potential to change the way present WCD systems construct cosmic ray trajectories with muons, by providing a very accurate, efficient, reliable, and economically viable method to the WCD community. It is based on a very intuitive phenomenon and is aimed toward the next generation of Cherenkov detectors. If implemented, this technique will reduce the number of PMTs currently used in water-based Cherenkov detectors. This can further play a phenomenal role in the reconstruction of air showers as well by constraining the shower trajectory with IACTs.

I thank Robert J. Nemiroff for valuable feedback and direction, and the anonymous referee for critical comments.

ORCID iDs

Neerav Kaushal  <https://orcid.org/0000-0003-4786-2348>

References

- Aab, A., Abreu, P., Aglietta, M., et al. 2015, *ApJ*, **802**, 111
- Aartsen, M. G., Ackermann, M., Adams, J., et al. 2017, *JInst*, **12**, P03012
- Arisaka, K., Kajita, T., Kifune, T., et al. 1984, in *AIP Conf. Proc.* 114, Low Energy Tests of Conservation Laws in Particle Physics, ed. M. Blecher & K. Gotow (Melville, NY: AIP), 54
- BenZvi, S. 2015, *EPJWC*, **105**, 01003
- Cavaliere, A., Morrison, P., & Sartori, L. 1971, *Sci*, **173**, 525
- Čerenkov, P. A. 1937, *PhRv*, **52**, 378
- Clerici, M., Spalding, G. C., Warburton, R., et al. 2016, *SciA*, **2**, e1501691
- Dingus, B. L. 2007, in *AIP Conf. Proc.* 912, The First GLAST Symp., ed. S. Ritz, P. Michelson, & C. A. Meegan (Melville, NY: AIP), 438
- Faccio, D., & Velten, A. 2018, *RPPH*, **81**, 105901

- Hakkila, J., & Nemiroff, R. 2019, *ApJ*, **883**, 70
- Huentemeyer, P., Matthews, J. A. J., & Dingus, B. 2009, arXiv:0909.2830
- Joshi, V. 2019, PhD Thesis, Heidelberg Univ., doi:10.11588/heidok.00026062
- Kaushal, N., & Nemiroff, R. J. 2020, RID: Relativistic Image Doubling in Water Cherenkov Detectors, 001, Astrophysics Source Code Library, ascl:2005.001
- Kaushal, N., & Nemiroff, R. J. 2020, *ApJ*, **898**, 53
- Milnes, J. S., Horsfield, C. J., Rubery, M. S., Glebov, V. Yu., & Herrmann, H. W. 2012, *RSci*, **83**, 10D301
- Nemiroff, R. 2019, AAS Meeting, **233**, #251.01
- Nemiroff, R. J. 2015, *PASA*, **32**, e001
- Nemiroff, R. J. 2018, *AnP*, **530**, 1700333
- Nemiroff, R. J., & Kaushal, N. 2020, *ApJ*, **889**, 122
- Nomerotski, A. 2019, *NIMPA*, **937**, 26
- Rossi, B. 1933, *ZPhy*, **82**, 151
- Sandoval, A. 2013, ICRC (Rio de Janeiro), **33**, 1155
- Tanabashi, M., Hagiwara, K., Hikasa, K., et al. 2018, *PhRvD*, **98**, 030001
- Velten, A., Wu, D., Jarabo, A., et al. 2013, *ACM Trans. Graph.*, **32**, 1
- Wisher, I. G. 2016, PhD Thesis, Univ. of Wisconsin-Madison